

Supporting Information

Low-carbon co-disposal of municipal sludge with sintered brick materials: Kinetics and emission control

Peng Lu ¹, Guanyuan Zhang ¹, Lyumeng Ye ^{1,*}, Jianjun Chen ^{2,*}, Chaoping Cen ¹

1. Guangdong Province Engineering Laboratory for Air Pollution Control, Guangdong Provincial Key Laboratory of Water and Air Pollution Control, South China Institute of Environmental Sciences, MEE, Guangzhou 510655, China

2. State Key Joint Laboratory of Environment Simulation and Pollution Control, School of Environment, Tsinghua University, Beijing 100084, China

*Corresponding authors:

L. Ye. E-mail: yelvmeng@scies.org.

J. Chen. E-mail: chenjianjun@tsinghua.edu.cn.

Kinetic analysis was conducted to determine the kinetic parameters of individual samples and blends. The general form of the kinetic equation for heterogeneous solid-phase reactions based on the Arrhenius law is expressed as:

$$\frac{d\alpha}{dt} = k(T) \cdot f(\alpha) \quad (\text{S1})$$

where α , t , T , $k(T)$, and $f(\alpha)$ represent conversion rate (%), reaction time (min), absolute temperature (K), reaction rate constant, and reaction mechanism function, respectively. The conversion rate (α) and rate constant $k(T)$ are defined as:

$$\alpha = \frac{m_0 - m_t}{m_0 - m_\infty} \quad (\text{S2})$$

$$k(T) = A \exp\left(-\frac{E}{RT}\right) \quad (\text{S3})$$

Here, m_0 , m_t , and m_∞ denote the initial, instantaneous, and final sample mass, respectively; E_a is the apparent activation energy ($\text{kJ} \cdot \text{mol}^{-1}$), A is apparent pre-exponential factor (min^{-1}) and R is the universal gas constant (8.314 J/K mol).

For thermogravimetric analysis with linear heating, heating rate β is defined as:

$$\beta = \frac{dT}{dt} \quad (\text{S4})$$

Combined with **Eqs. (S1), (S3) and (S4)**, the chemical reaction kinetic equation of constant heating rate can be obtained as follow:

$$\frac{d\alpha}{dT} = \frac{A}{\beta} \exp\left(-\frac{E}{RT}\right) f(\alpha) \quad (\text{S5})$$

Integration of **Eq. (S5)** under initial conditions ($\alpha = 0$ at $T = T_0$) gives the fundamental integral form for kinetic analysis:

$$\int_0^\alpha \frac{d\alpha}{f(\alpha)} = \frac{A}{\beta} \int_{T_0}^T \exp\left(-\frac{E}{RT}\right) dT \quad (\text{S6})$$

The apparent activation energy (E_a) was evaluated using two model-free methods - Flynn-Wall-Ozawa (FWO) and Kissinger-Akahira-Sunose (KAS) - along with the

Coats-Redfern (C-R) integral method, with validation against the master plots approach.

(1) Model-free methods

The FWO method was derived from Doyle's approximation with Eq. (S6) as follows:

$$\ln \beta = \ln \left[\frac{AE}{RG(\alpha)} \right] - 5.331 - 1.052 \frac{E}{RT} \quad (\text{S7})$$

The KAS method, based on the Coats-Redfern approximation $p(x) = x^{-2}e^{-x}$, takes the form:

$$G(\alpha) = \ln \left(\frac{\beta}{T^2} \right) = \ln \left[\frac{AR}{EG(\alpha)} \right] - \frac{E}{RT} \quad (\text{S8})$$

For constant conversion α , E_a is determined from the slope ($-E_a/R$) of linear plots of $\ln \beta$ versus $1/T$ (FWO) or $\ln \left(\frac{\beta}{T^2} \right)$ versus $1/T$ (KAS).

(2) Coats-Redfern Integral Method

Unlike model-free methods requiring multiple heating rates, the C-R method enables kinetic parameter estimation from single heating rate data:

$$\ln \left[-\frac{\ln(1-\alpha)}{T^2} \right] = \ln \left[\frac{AR}{\beta E} \left(1 - \frac{2RT}{E} \right) \right] - \frac{E}{RT} \quad (n=1) \quad (\text{S9})$$

$$\ln \left[\frac{1-(1-\alpha)^{1-n}}{T^2(1-n)} \right] = \ln \left[\frac{AR}{\beta E} \right] - \frac{E}{RT} \quad (n \neq 1) \quad (\text{S10})$$

(3) Master Plots Method

The most reliable E_a values from model-free analyses were used with the master plots method to identify optimal kinetic models. Integrating Eq. (S6) gives:

$$G(\alpha) = \frac{AE_a}{\beta R} P(u) \quad (\text{S11})$$

where $u = E_a/RT$ and $P(u)$ represent the temperature integral. Using the empirical approximation:

$$P(u) = \frac{\exp(-u)}{u \times (1.00198882u + 1.87391198)} \quad (\text{S12})$$

Taking $\alpha = 0.5$ as reference:

$$G(0.5) = \frac{AE_a}{\beta R} P(u_{0.5}) \quad (\text{S13})$$

Division of equation (S11) by (S13) yields the master plot equation:

$$\frac{G(\alpha)}{G(0.5)} = \frac{P(u)}{P(u_{0.5})} \quad (\text{S13})$$

In order to obtain the best kinetic model, various common $G(\alpha)$ functions (**Table S1**) were used and the theoretical master plots of $G(\alpha)/G(0.5)$ as a function of α were plotted. The experimental main plot of $P(u)/P(u_{0.5})$ versus α was also plotted based on the thermogravimetric data obtained at different heating rates. From **Eq. (S13)**, it can be seen that for a given x , the values of $P(u)/P(u_{0.5})$ and $G(\alpha)/G(0.5)$ are equal. Therefore, the higher the agreement between theoretical and experimental data, the most appropriate kinetic model represented by this function. Otherwise, when an unsuitable $G(\alpha)$ kinetic model is used, the theoretical and experimental main plots will deviate significantly.

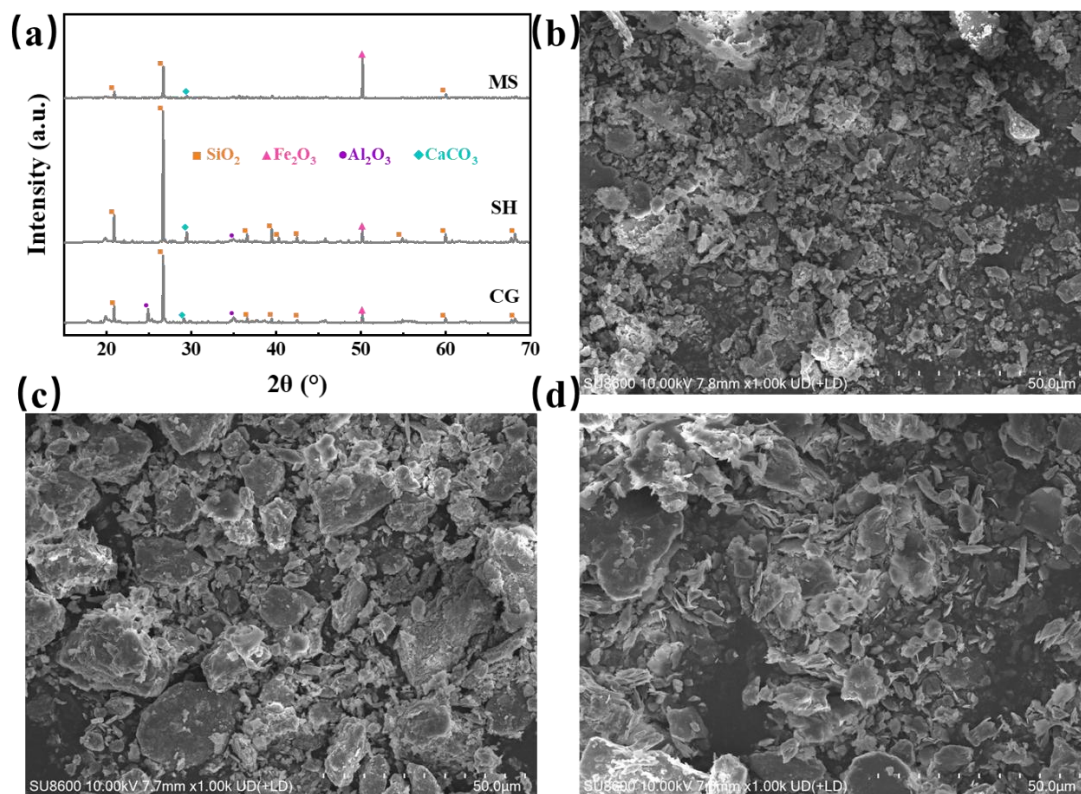


Fig. S1 (a) XRD patterns of materials, SEM images of (b) MS, (c) SH, and (d) CG.

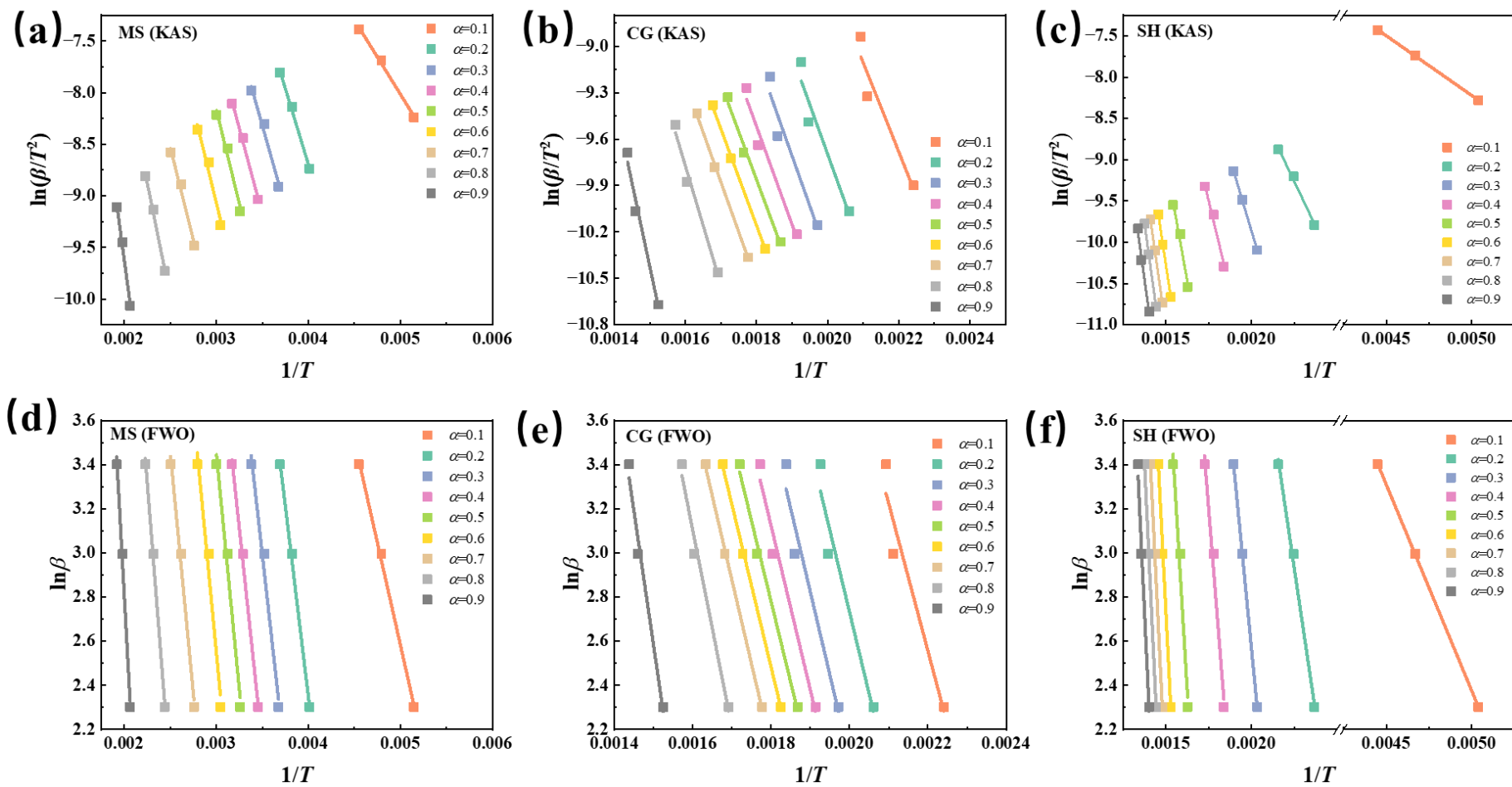


Fig. S2 E_a estimation and fitting curves of MS, SH and CG combustion in oxidizing atmosphere based on FWO and KAS methods.

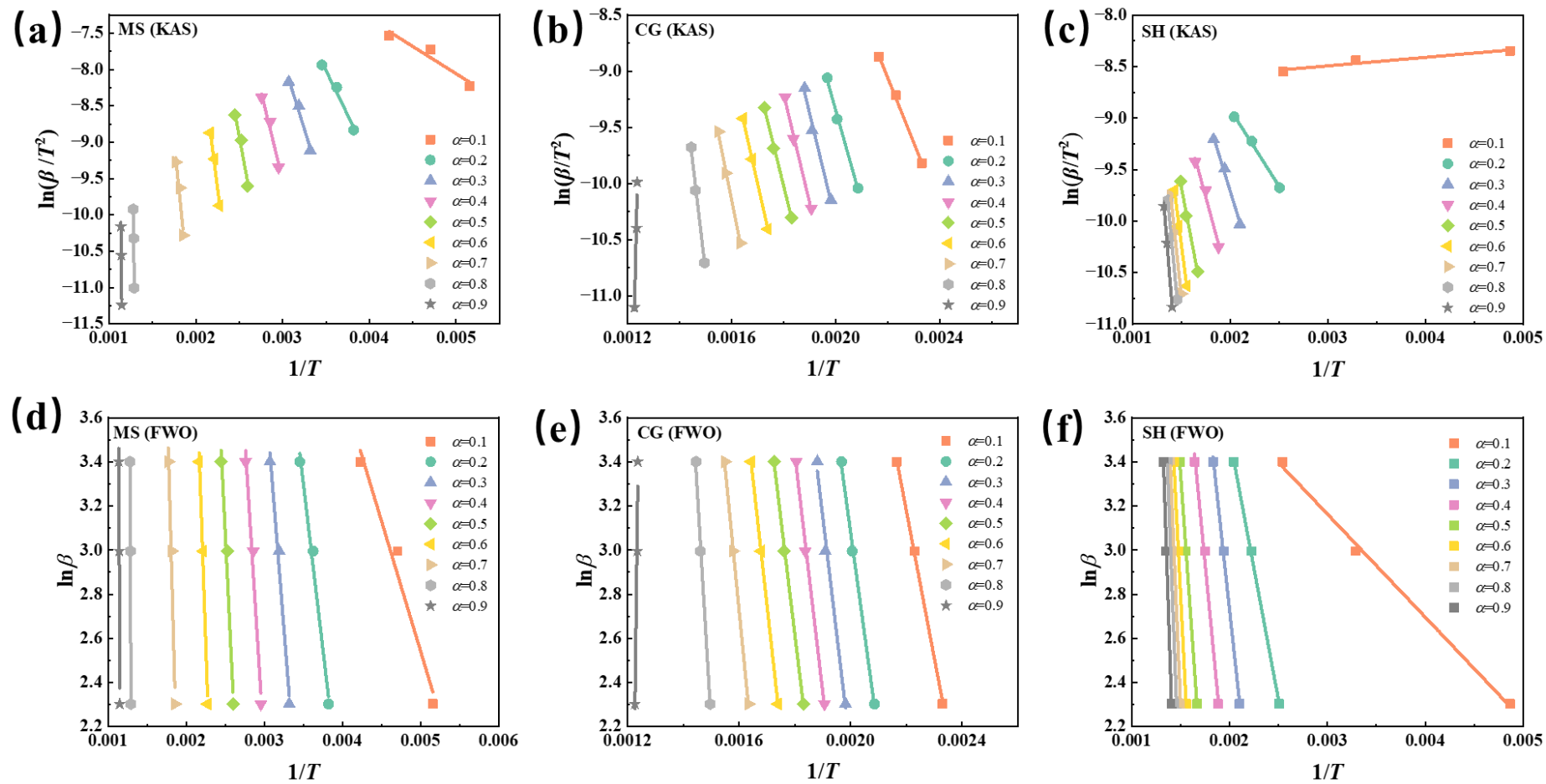


Fig. S3 E_a estimation and fitting curves of MS, SH and CG pyrolysis in inert atmosphere based on FWO and KAS methods.

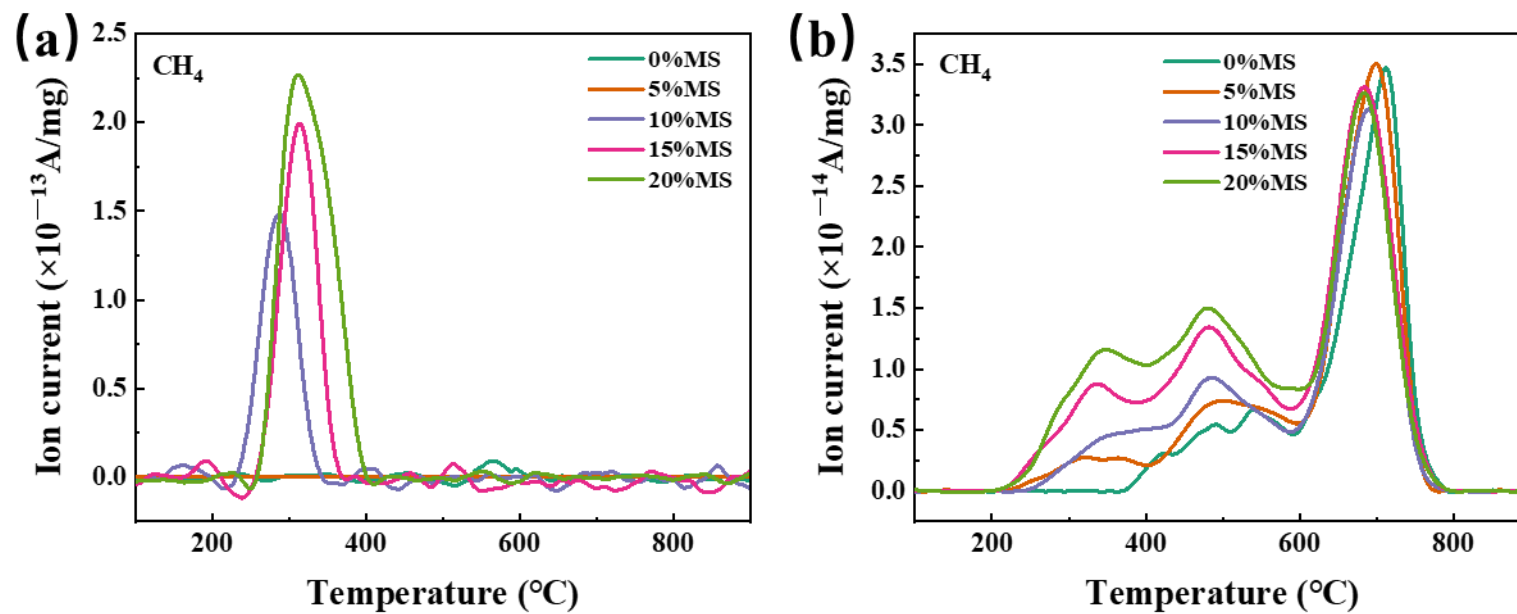


Fig. S4 Variation curves of CH₄ ionic strength of mixed samples in oxidizing (a) and inert (b) atmospheres.

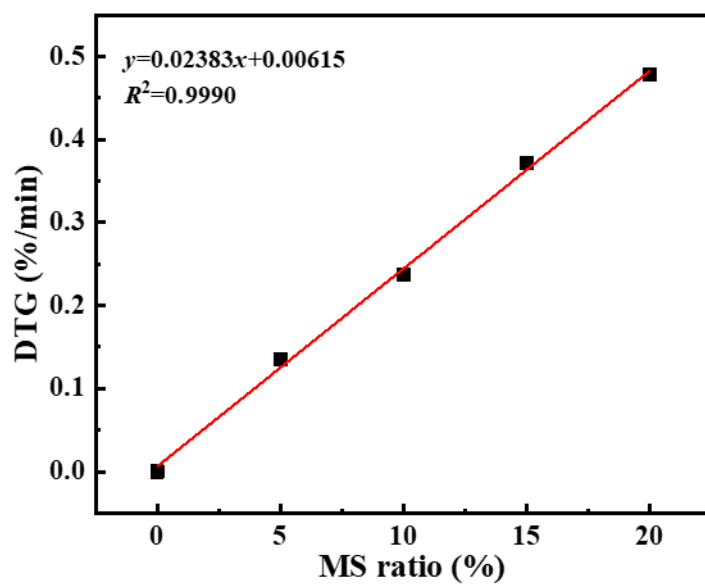


Fig. S5 Graph showing the relationship between the proportion of sludge incineration and the intensity of characteristic peaks in the low-temperature zone.

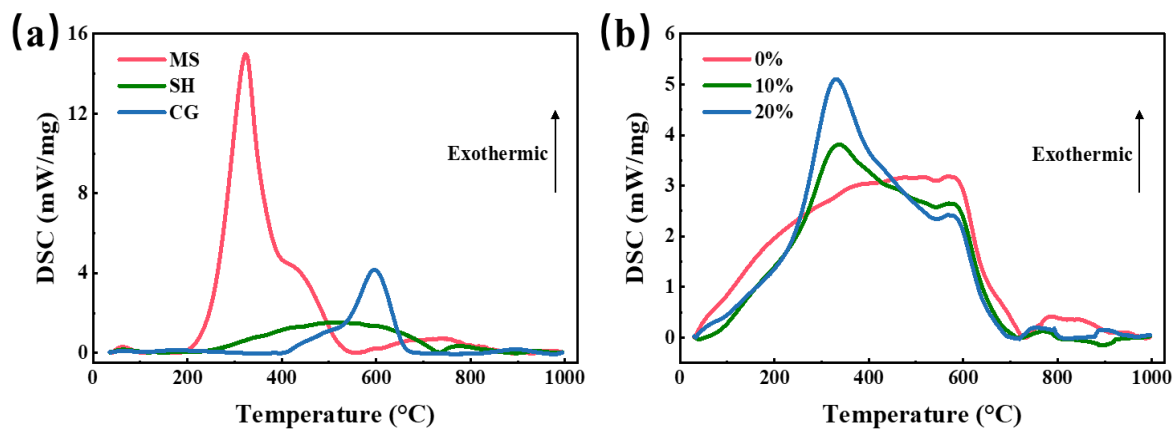


Fig. S6 DSC curves of (a) MS, CG and SH combustion and (b) blends combustion at a heating rate of 30 °C/min.

Table S1 The most common kinetic models and their corresponding mechanisms

Reaction model	Code	$f(\alpha)$	$G(\alpha)$
<i>Diffusion</i>			
One-way transport	D1	$1/(2\alpha)$	α^2
Two-way transport	D2	$[-\ln(1-\alpha)]^{-1}$	$(1-\alpha)\ln(1-\alpha)+\alpha$
Three-way transport	D3	$(3/2)(1-\alpha)^{2/3}[1-(1-\alpha)^{1/3}]^{-1}$	$[1-(1-\alpha)^{1/3}]^2$
Ginstling–Brounshtein equation	D4	$(3/2)[(1-\alpha)^{-1/3}-1]^{-1}$	$(1-2\alpha/3)-(1-\alpha)^{2/3}$
<i>Reaction order models</i>			
First-order	F1	$1-\alpha$	$-\ln(1-\alpha)$
Second-order	F2	$(1-\alpha)^2$	$(1-\alpha)^{-1}-1$
Third-order	F3	$(1-\alpha)^3$	$[(1-\alpha)^{-2}-1]/2$
Fourth-order	F4	$(1-\alpha)^4$	$[(1-\alpha)^{-3}-1]/3$
<i>Nucleation growth model</i>			
Avrami-Erofeev	A1	$(1/2)(1-\alpha)[-\ln(1-\alpha)]^{1/3}$	$[-\ln(1-\alpha)]^{2/3}$
One point five-dimensional	A1.5	$1.5(1-\alpha)[-\ln(1-\alpha)]^{1/3}$	$[-\ln(1-\alpha)]^{2/3}$
Two-dimensional	A2	$2(1-\alpha)[-\ln(1-\alpha)]^{1/2}$	$[-\ln(1-\alpha)]^{1/2}$
Three-dimensional	A3	$3(1-\alpha)[-\ln(1-\alpha)]^{2/3}$	$[-\ln(1-\alpha)]^{1/3}$
<i>Exponential nucleation</i>			
Power law	P2	$2\alpha^{2/3}$	$\alpha^{1/2}$
Power law	P3	$3\alpha^{2/3}$	$\alpha^{1/3}$
Index law	P4	$4\alpha^{3/4}$	$\alpha^{1/4}$
<i>Geometrical contraction models</i>			
One dimension	R1	1	α
Two dimensions	R2	$2(1-\alpha)^{1/2}$	$1-(1-\alpha)^{1/2}$
Three dimensions	R3	$3(1-\alpha)^{2/3}$	$1-(1-\alpha)^{1/3}$

Table S2 Stage classification of MS, CG and SH and their mass losses at three heating rates in oxidizing atmosphere

Samples	β (°C/min)	Stage 1		Stage 2		Stage 3		Stage 4		Total
		Temperature	Weight	Temperature	Weight	Temperature	Weight	Temperature	Weight	Weight
		Range/ (°C)	Loss / (%)	Range / (°C)	Loss / (%)	Range / (°C)	Loss / (%)	Range / (°C)	Loss / (%)	Loss / (%)
MS	10	50–185	3.32	185–730	31.74	730–1000	1.25	/	/	36.31
	20	50–190	3.03	190–775	32.62	775–1000	1.12	/	/	36.77
	30	50–200	2.95	200–810	32.75	810–1000	1.02	/	/	36.72
CG	10	50–265	0.56	265–855	9.96	855–1000	0.09	/	/	10.61
	20	50–270	0.20	270–885	10.38	885–1000	0.06	/	/	10.64
	30	50–280	0.46	280–900	10.29	900–1000	0.09	/	/	10.84
SH	10	50–225	0.84	225–590	2.88	590–820	4.05	820–1000	0.22	7.99
	20	50–265	0.89	265–605	2.59	600–880	4.09	880–1000	0.21	7.78
	30	50–300	0.90	300–615	2.47	615–910	4.07	910–1000	0.04	7.48

Table S3 Pyrolysis stage classification of MS, CG and SH and their mass losses at three heating rates in inert atmosphere

Samples	Heating Rate/ (°C/min)	Stage 1		Stage 2		Stage 3		Stage 4		Total
		Temperature Range/ (°C)	Weight Loss / (%)	Temperature Range / (°C)	Weight Loss / (%)	Temperature Range / (°C)	Weight Loss / (%)	Temperature Range / (°C)	Weight Loss / (%)	Weight Loss / (%)
MS	10	50–160	2.81	160–570	26.47	570–1000	11.92	/	/	41.20
	20	50–170	2.54	170–600	26.74	600–1000	11.36	/	/	40.64
	30	50–180	1.77	175–620	26.62	620–1000	10.85	/	/	39.24
CG	10	50–270	0.35	270–805	6.84	805–1000	0.85	/	/	8.04
	20	50–285	0.28	285–830	7.11	830–1000	0.75	/	/	8.14
	30	50–325	0.37	325–825	6.83	825–1000	0.74	/	/	7.94
SH	10	50–180	0.92	180–580	3.63	580–775	4.56	775–1000	0.50	9.61
	20	50–255	0.73	255–590	2.45	590–825	4.04	825–1000	0.34	7.56
	30	50–250	0.48	250–620	2.47	620–865	4.02	865–1000	0.04	7.15

Table S4 E_a estimation and R^2 of MS, CG and SH in oxidizing atmosphere

Samples	α	KAS			FWO		
		$y=ax + b$	$E/$ (KJ/mol)	R^2	$y=ax + b$	$E/$ (KJ/mol)	R^2
MS	0.1	$y = -1441.72 x - 0.81$	11.99	0.9957	$y = -1854.18 x - 11.85$	14.65	0.9978
	0.2	$y = -2932.67 x - 3.04$	24.38	0.9968	$y = -3451.84 x + 16.16$	27.28	0.9978
	0.3	$y = -3162.60 x - 2.75$	26.29	0.9798	$y = -3729.71 x + 16.05$	29.48	0.9859
	0.4	$y = -3317.63 x - 2.44$	27.58	0.9958	$y = -3921.13 x + 15.86$	30.99	0.9972
	0.5	$y = -3645.01 x - 2.77$	30.3	0.9746	$y = -4284.12 x + 16.31$	33.86	0.9820
	0.6	$y = -3672.84 x - 1.95$	30.54	0.9602	$y = -4358.60 x + 15.63$	34.45	0.9720
	0.7	$y = -3599.82 x - 0.47$	29.93	0.9832	$y = -4360.14 x + 14.36$	34.46	0.9890
	0.8	$y = -4410.44 x - 1.05$	36.67	0.9923	$y = -5266.97 x + 15.17$	41.63	0.9949
	0.9	$y = -6607.36 x - 3.60$	54.93	0.9878	$y = -7611.91 x + 18.04$	60.16	0.9911
	Average		30.29	0.9851		34.11	0.9897
CG	0.1	$y = -5759.15 x - 2.99$	47.88	0.9141	$y = -6680.95 x + 17.25$	52.80	0.9345
	0.2	$y = -6383.69 x - 3.07$	53.07	0.9260	$y = -7385.69 x + 17.50$	58.37	0.9434
	0.3	$y = -6487.07 x + 2.62$	53.93	0.9353	$y = -7535.38 x + 17.14$	59.55	0.9509

	0.4	$y = -6351.6x + 1.91$	52.81	0.9690	$y = -7435.09x + 16.51$	58.76	0.9769
	0.5	$y = -6195.5x + 1.29$	51.51	0.9916	$y = -7308.86x + 15.93$	57.76	0.9938
	0.6	$y = -6230.6x + 1.06$	51.80	0.9989	$y = -7371.18x + 15.75$	58.25	0.9991
	0.7	$y = -6430.85x + 1.05$	53.47	0.9987	$y = -7602.53x + 15.80$	60.08	0.9989
	0.8	$y = -7705.02x + 2.55$	64.06	0.9831	$y = -8928.44x + 17.39$	70.56	0.9871
	0.9	$y = -10812.81x + 5.79$	89.90	0.9780	$y = -12161.3x + 20.82$	96.11	0.9824
	Average		57.60	0.9661		63.58	0.9741
SH	0.1	$y = -1446.51x - 0.99$	12.03	0.9999	$y = -1867.66x + 11.71$	14.76	1
	0.2	$y = -4350.97x + 0.53$	36.17	0.9948	$y = -5234.54x + 14.71$	41.37	0.9965
	0.3	$y = -6950.45x + 4.04$	57.79	0.9998	$y = -7967.71x + 18.51$	62.97	0.9998
	0.4	$y = -8578.40x + 5.52$	71.32	0.9831	$y = -9700.67x + 20.18$	76.66	0.9870
	0.5	$y = -11564.08x + 8.32$	96.14	0.9755	$y = -12826.85x + 23.22$	101.37	0.9802
	0.6	$y = -13796.23x + 10.42$	114.7	0.9999	$y = -15135.50x + 25.43$	119.62	0.9999
	0.7	$y = -14482.66x + 10.68$	120.41	0.9996	$y = -15866.18x + 25.76$	125.39	0.9997
	0.8	$y = -14892.62x + 10.70$	123.82	0.9979	$y = -16310.44x + 25.82$	128.9	0.9982
	0.9	$y = -14997.81x + 10.17$	124.69	0.9830	$y = -16456.57x + 25.35$	130.06	0.9858
	Average		84.12	0.9926		89.01	0.9941

Table S5 E_a estimation and R^2 for MS, CG and SH in inert atmosphere

Samples	α	KAS			FWO		
		$y=ax + b$	$E/$ (KJ/mol)	R^2	$y=ax + b$	$E/$ (KJ/mol)	R^2
MS	0.1	$y = -750.36 x - 4.3$	6.24	0.9268	$y = -1178.23 x + 8.43$	9.31	0.9723
	0.2	$y = -2449.25 x + 0.56$	20.36	0.9813	$y = -2999.32 x + 13.80$	23.7	0.9880
	0.3	$y = -3820.93 x + 3.6$	31.77	0.9798	$y = -4447.16 x + 17.10$	35.15	0.9854
	0.4	$y = -4899.11 x + 5.18$	40.73	0.9680	$y = -5599.77 x + 18.89$	44.26	0.9757
	0.5	$y = -6457.2 x + 7.22$	53.69	0.9655	$y = -7250.68 x + 21.19$	57.3	0.9727
	0.6	$y = -9352.9 x + 11.41$	77.76	0.9822	$y = -10254.76 x + 25.63$	81.04	0.9853
	0.7	$y = -11894.73 x + 11.82$	98.89	0.9446	$y = -13000.36 x + 26.45$	102.74	0.9534
	0.8	$y = -104060.03 x + 123.13$	865.16	0.9996	$y = -105617.50 x + 138.45$	834.7	0.9996
	0.9	$y = -103555.99 x + 107.44$	860.96	0.9563	$y = -105310.16 x + 123.00$	832.27	0.9577
	Average		228.40	0.9671		224.50	0.9767
CG	0.1	$y = -5772.62 x + 3.64$	47.99	0.9984	$y = -6661.67 x + 17.84$	52.65	0.9989
	0.2	$y = -8230.86 x + 7.12$	68.43	0.9964	$y = -9216.28 x + 21.52$	72.84	0.9971
	0.3	$y = -9592.81 x + 8.85$	79.75	0.9888	$y = -10626.9 x + 23.35$	83.99	0.9908
	0.4	$y = -9691.47 x + 8.24$	80.57	0.9956	$y = -10767.64 x + 22.82$	85.10	0.9964

	0.5	$y = -9321.33 x + 6.76$	77.50	0.9989	$y = -10444.37 x + 21.42$	82.54	0.9991
	0.6	$y = -10242.23 x + 7.41$	85.15	1	$y = -11423.44 x + 22.18$	90.28	1
	0.7	$y = -11648.81 x + 8.50$	96.85	0.998	$y = -12903.9 x + 23.38$	101.98	0.9983
	0.8	$y = -19708.47 x + 18.79$	163.86	0.9958	$y = -21066.78 x + 33.83$	166.49	0.9963
	0.9	$y = -97857.81 x - 131.17$	813.59	0.9520	$y = -96234.02 x - 115.77$	760.54	0.9505
	Average		168.19	0.9915		166.27	0.9919
	0.1	$y = 82.76 x - 8.74$	-0.69	0.9376	$y = -466.45 x + 4.56$	3.69	0.9971
	0.2	$y = -1494.29 x - 5.93$	12.42	0.9976	$y = -2374.15 x + 8.25$	18.76	0.9996
	0.3	$y = -3079.07 x - 3.55$	25.6	0.9927	$y = -4097.58 x + 10.92$	32.38	0.9965
	0.4	$y = -3477.10 x - 3.69$	28.91	0.9814	$y = -4614.34 x + 11.00$	36.47	0.9903
SH	0.5	$y = -4970.09 x - 2.22$	41.32	0.9949	$y = -6234.32 x + 12.68$	49.27	0.9964
	0.6	$y = -7383.69 x + 0.84$	61.39	0.9965	$y = -8721.63 x + 15.85$	68.93	0.9973
	0.7	$y = -8953.26 x + 2.69$	74.44	0.9975	$y = -10336.17 x + 17.77$	81.69	0.9981
	0.8	$y = -10097.13 x + 3.93$	83.95	0.9986	$y = -11515.42 x + 19.06$	91.01	0.9989
	0.9	$y = -11899.89 x + 5.87$	98.94	1	$y = -13366.13 x + 21.07$	105.63	1
	Average		47.36	0.9885		54.20	0.9971

Table S6 Stage classification of MS, SH and CG and their mass losses at three heating rates in oxidizing atmosphere

Samples	Stage 1		Stage 2		Stage 3		Stage 4		Total Weight Loss / (%)
	Temperature Range/ (°C)	Weight Loss / (%)	Temperature Range/ (°C)	Weight Loss / (%)	Temperature Range/ (°C)	Weight Loss / (%)	Temperature Range/ (°C)	Weight Loss / (%)	
MS	50–190	3.53	190–750	32.17	750–1000	1.07	/	/	36.73
CG	50–280	0.51	280–880	10.23	880–1000	0.13	/	/	10.87
SH	50–245	0.54	245–600	2.54	600–820	3.70	820–1000	0.07	6.85
SH80CG20	50–215	0.51	215–620	3.38	620–1000	2.73	/	/	6.62
MS5SH75CG20	50–200	0.71	200–405	1.69	405–615	3.56	615–1000	3.04	9.00
MS10SH70CG20	50–190	0.77	190–425	2.00	245–615	3.74	615–1000	2.99	10.50
MS15SH65CG20	50–190	0.80	190–450	4.40	450–615	3.66	615–1000	2.89	11.75
MS20SH60CG20	50–190	1.03	190–450	5.89	450–615	3.56	615–1000	2.52	13.02

Table S7 Pyrolysis stage division and mass loss of mixed samples in inert atmosphere

Samples	Stage 1		Stage 2		Stage 3		Stage 4		Stage 5	
	Temperature Range/ (°C)	Weight Loss / (%)	Temperature Range/ (°C)	Weight Loss / (%)	Temperature Range/ (°C)	Weight Loss / (%)	Temperature Range/ (°C)	Weight Loss / (%)	Temperature Range/ (°C)	Weight Loss / (%)
MS	50–175	3.06	175–610	27.33	610–1000	11.28	/	/	/	/
CG	50–275	0.50	275–845	6.97	845–1000	0.60	/	/	/	/
SH	50–270	0.87	270–570	2.19	570–825	4.60	825–1000	0.38	/	/
SH80CG20	50–275	0.23	275–600	2.55	600–890	3.31	890–1000	0.05	/	/
MS5SH75CG20	50–205	0.82	205–600	4.06	600–800	3.54	800–1000	0.59	/	/
MS10SH70CG20	50–190	0.81	190–600	5.31	600–780	3.42	780–1000	1.10	/	/
MS15SH65CG20	50–190	0.97	190–405	2.78	405–600	3.72	600–835	3.81	835–1000	1.15
MS20SH60CG20	50–190	0.94	190–400	3.77	400–600	4.07	600–855	4.16	855–1000	1.37